

International Conference on Computational Science, ICCS 2012

## Multiphysics Modeling and Simulation of Fluid-structure interaction applied to biological problems

Felix Mihai<sup>a</sup>, Inja Youn<sup>b</sup>, Padmanabhan Seshaiyer<sup>c,\*</sup>

<sup>a</sup>College of Science, George Mason University, Fairfax, VA 22030

<sup>b</sup>Department of Computer Science, George Mason University, Fairfax, VA 22030

<sup>c</sup>Department of Mathematical Sciences, George Mason University, Fairfax, VA 22030

---

### Abstract

In this paper, we consider the mathematical modeling and simulation of a fluid-structure interaction algorithm applied to a multiphysics application involving atherosclerotic arteries which is known to lead to health risks and mortality. More specifically, narrowing of an artery that can result from a plaque deposit causes severe reduction of the blood flow. Modeling such diseased arteries requires modeling the unsteady blood flow interacting with the compliant arterial vessel wall as well as a plaque in an efficient way. In this work, we will present a comprehensive model of these multi-physics phenomena that incorporates both geometric nonlinearity and material nonlinearity for the arterial wall and a non-axisymmetric plaque that interacts with unsteady blood flow. In particular, these models indicate the generation of recirculation zones at various locations near the plaque which could potentially enhance the risk of the formation of a clot. In particular, our results indicate the importance of incorporating nonlinearity both in the material and geometry in the modeling.

"Keywords: Fluid-Structure Interaction; Multiphysics; Atherosclerosis"

---

### 1. Introduction

In the last decade, the rapid development of computational science has provided new methodologies to solve complex multiphysics applications involving fluid-structure interaction to a variety of fields. These include solving applications involving blood flow interactions with the arterial wall to computational aeroelasticity of flexible wing micro-air vehicles. In these applications, the challenge is to understand and develop algorithms that allow the structural deformation and the flow field to interact in a highly non-linear fashion. Not only is the non-linearity in the geometry challenging but in many of these applications the material is non-linear as well that makes the problem even more complex. Direct numerical solution of the highly non-linear equations governing even the most simplified two-dimensional models of such fluid-structure interaction, requires that both the flow field and the

---

\* Corresponding author. Tel.: +1-703-993-9787; fax: +1-703-993-1491.  
E-mail address: [pseshaiy@gmu.edu](mailto:pseshaiy@gmu.edu).

domain shape be determined as part of the solution, since neither is known a priori.

The past few decades, however, have seen significant advances in the development of iterative methods. Coupled with advances in finite element methods and domain decomposition methods, these have provided new algorithms for such large scale multiphysics simulations. There have been several methods that have been introduced in this regard and their performance has been analyzed for a variety of problems. One such technique is the mortar finite element method which has been shown to be stable mathematically and has been successfully applied to a variety of applications [1, 2, 3, 4, 5, 6 and references therein]. The basic idea is to replace the strong continuity condition at the interfaces between the different subdomains modeling different multiphysics by a weaker one to solve the problem in a coupled fashion. Such novel techniques provide hope for us to develop new faster and efficient algorithms to solve complex fluid-structure applications. A variety of methods have been introduced including the level set methods [7], the fictitious domain methods [8, 9], non-conforming hp finite element methods [4, 10], multilevel multigrid methods [11] and the immersed boundary methods [12]. While these methods help enhance our ability to understand complex processes (such as the interaction of blood flow with the arterial wall), when used in conjunction with traditional MRI and CT scan image reconstruction tools, there is still a great need for efficient computational methods that can not only help simulate physiologically realistic situations qualitatively but also analyze and study patient-specific modeling of such processes quantitatively.

Cardiovascular atherosclerotic arteries that often consist of diseased plaques are known to be the leading cause of health risks and mortality. More specifically, narrowing of an artery that can result from a plaque deposit causes severe reduction of the blood flow. Modeling such diseased arteries requires modeling the unsteady blood flow interacting with the compliant arterial vessel wall as well as a plaque in an efficient way. It is well known that the presence of a plaque can significantly alter the characteristics of the blood flow in arteries which can then lead to the development of cardiovascular atherosclerotic disease. In current clinical practice, the degree of the luminal narrowing determines the need to surgically remove an existing plaque [13]. The Doppler ultrasound technique that is currently employed uses the maximum peak systolic and diastolic blood flow velocities as well as the spectral composition of these velocities. Although this technique is in universal clinical use, there have been problems in the use of this technique. Moreover, due to the nature of the associated strong coupling of the plaque with the blood flow and arterial wall, there is a great need to develop coupled models to understand the displacement of the plaque and its interaction with the flow. These often results in recirculation zones around the plaque that lead to the formation of a thrombus, that eventually leads to a heart attack or a stroke.

To estimate the stress levels on the plaque surface, fluid structure interaction analysis has emerged as an efficient computational tool that has combined computational fluid dynamics for the blood with structural mechanics of the surrounding elements such as the arterial wall and the plaque [14, 15]. In these papers, the authors conducted a finite element analysis to examine the fluid structure interaction of pulsatile and unsteady flow through a compliant stenotic artery respectively. They both observed complex flow patterns and high shear stress at the throat of the plaque and their results indicated critical plaque stress/strain conditions are influenced by a variety of biomechanical factors. Most of the prior simulations have used a geometrically linear material approximation. There is a lot of evidence and experimental results that suggest that soft tissues undergo large deformations (which cannot be modeled via an infinitesimal deformation) that make them *geometric nonlinear* structures. Hence the nonlinear terms play an essential role in understanding the failure of a structure which brings us to the focus of this work.

The *focus of this paper* will therefore be to present and apply a coupled fluid-structure interaction algorithm to simulate a biological application that involves both geometric and material non-linearity. In particular, we will present the mathematical modeling and simulation of a fluid-structure interaction algorithm applied to a multiphysics application involving atherosclerotic arteries. More specifically, we will present a comprehensive model of these multi-physics phenomena that incorporates both geometric nonlinearity and material nonlinearity for the arterial wall and the plaque that interact with unsteady blood flow. In particular, these models indicate the generation of recirculation zones at various locations near the plaque which could potentially enhance the risk of the formation of a clot. The outline of the paper is as follows. We first describe the mathematical model and the associated governing equations for a model problem. This is divided into three parts, the model for the fluid components, the structural components and the coupled fluid-structure model. The numerical section then presents the performance of these models in the presence of various types of non-linearities and the influence they have on the parameters of interest.

## 2. Mathematical Model and Governing equations

In this section, we will consider the multi-physics interaction of nonlinear structural domain interacting with an unsteady fluid medium. For simplicity of presentation, we consider the following computational model that involves multiple non-linear structural elements (arterial vessel walls and the plaque deposit) that interact with the unsteady blood flow. The computational domain is illustrated in Figure 1.

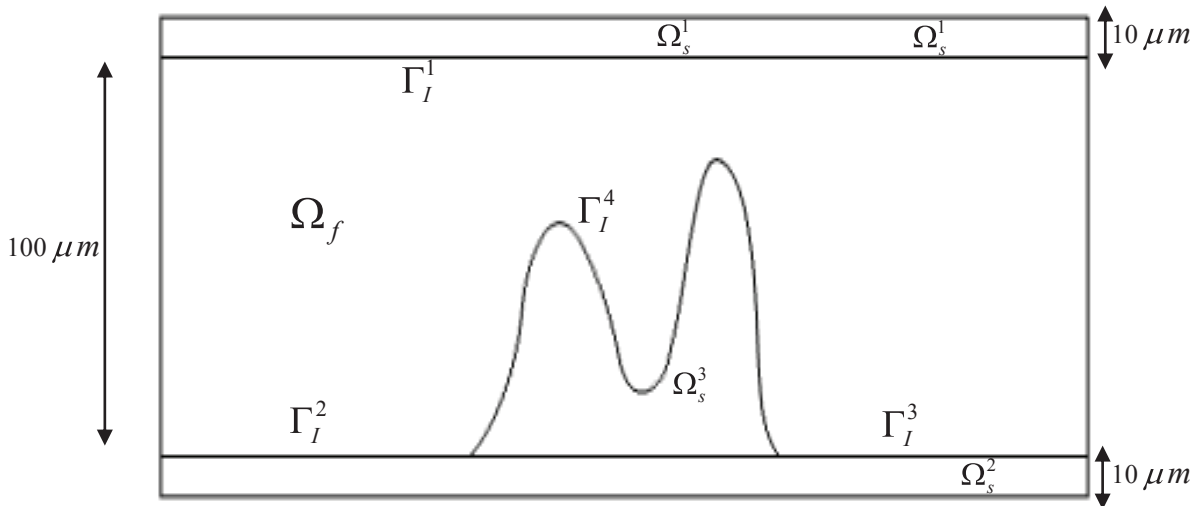


Figure 1. Computational Domain for the multiphysics problem

Let the computational domain  $\Omega \subset \mathbb{R}^2$  be an open set with global boundary  $\Gamma$ . Let  $\Omega$  be decomposed into the four disjoint open sets, a fluid subdomain  $\Omega_f$  and three solid subdomains  $\Omega_s^i, i = 1, 2, 3$  with respective boundaries  $\Gamma_f$  and  $\Gamma_s$ . Let  $\Gamma_I^j, j = 1, 2, 3, 4$  be the interface between the solid and fluid domains. The structural domain consists of two symmetric arterial vessel walls denoted by  $\Omega_s^1, \Omega_s^2$  and a domain describing the plaque  $\Omega_s^3$ .

### 2.1 Modelling the unsteady blood flow

We model the fluid domain via the unsteady Navier-Stokes equations for an incompressible, isothermal fluid flow written in non-conservative form as:

$$\begin{aligned} \rho_f \frac{\partial u_f}{\partial t} + \rho_f (u_f \cdot \nabla) u_f + \nabla p &= \nabla \cdot \tau_f + F_f \\ \rho_f \nabla \cdot u_f &= 0 \end{aligned} \tag{1}$$

where  $u_f$  is the fluid velocity,  $\rho_f$  is the fluid density,  $p$  is the pressure and  $F_f$  is the body forces. The viscous stress tensor  $\tau(u_f) = 2\eta D(u_f)$  where  $\eta$  is the dynamic viscosity and the deformation tensor is given by:

$$D(u_f) = \mu \left( \frac{\nabla u_f + (\nabla u_f)^T}{2} \right) \tag{2}$$

The fluid equations are subject to the boundary conditions:

$$\begin{aligned}
 u_f &= u_{wall}, & x \in \Gamma_I^j, j = 1,2,3,4 \\
 \tau_f \cdot n &= t \cdot n, & x \in \Gamma_N \\
 u_f &= \frac{\partial u_s}{\partial t}, & x \in \Gamma_I^j, j = 1,2,3,4
 \end{aligned}
 \tag{3}$$

where  $t = -pI + 2D(u_f)$  is the prescribed tractions on the Neumann part of the boundary with  $n$  being the outward unit normal vector to the boundary surface of the fluid. Conditions of displacement compatibility and force equilibrium along the structure-fluid interface are enforced.

The weak variational formulation of the fluid problem then becomes solving for the fluid velocity  $u_f$  and pressure  $p$  satisfying:

$$\begin{aligned}
 \int_{\Omega_f} \tau_f \cdot \nabla \phi \, d\Omega_f &= \int_{\Omega_f} F \cdot \phi \, d\Omega_f + \int_{\Omega_f} t \cdot \phi \, d\Omega_f - \int_{\Omega_f} \rho_f \frac{\partial u}{\partial t} \cdot \phi \, d\Omega_f - \int_{\Omega_f} \rho_f (u \cdot \nabla) u \cdot \phi \, d\Omega_f \\
 \int_{\Omega_f} q \nabla \cdot u \, d\Omega_f &= 0
 \end{aligned}
 \tag{4}$$

### 2.2 Modeling the Structure equations

The structural domains consists of the arterial vessel walls denoted by  $\Omega_s^1, \Omega_s^2$  and the plaque  $\Omega_s^3$ . They are modelled via the following equation:

$$\rho_s \frac{\partial^2 u_s}{\partial t^2} = \nabla \cdot \tau_s + F_s \tag{5}$$

where  $u_s$  is the structure displacement,  $\rho_s$  is the structure density,  $\tau_s$  is the solid stress tensor and  $\frac{\partial^2 u_s}{\partial t^2}$  is the local acceleration of the structure. This is solved with the boundary conditions:

$$\begin{aligned}
 u_s &= u_s^D & x \in \Gamma_S^D \\
 \tau_s \cdot n_s &= t_s & x \in \Gamma_S^N \\
 \tau_s \cdot n_s &= -\tau \cdot n + t_s^I & x \in \Gamma_I^j, j = 1,2,3,4
 \end{aligned}
 \tag{6}$$

Here  $\Gamma_S^D$  and  $\Gamma_S^N$  are the respective parts of the structural boundary where the Dirichlet and Neumann boundary conditions are prescribed. Also  $t_s$  are the applied tractions on  $\Gamma_S^N$  and  $t_s^I$  are the externally applied tractions to the interface boundaries  $\Gamma_I^j, j = 1,2,3,4$ . the unit outward normal vector to the boundary surface of the structure is  $n_s$ . The stresses are computed using the constitutive relations that will be described next. Equation (6) enforces the equilibrium of the traction between the fluid and the structure on the respective fluid-structure interfaces.

In continuum mechanics, there are two types of non-linearity that often arises in various applications. The first type is related to the constitutive law that dictates how the material responds to applied loads. This leads to a nonlinear relation between the stress  $\tau_s$  and the strain  $\epsilon$ . In this work, we consider two different constitutive models for the structural domains that include a linear elastic as well as a hyperelastic model. The second type of nonlinearity arises when the strain  $\epsilon$  varies nonlinearly with respect to the displacement. The total strain tensor for a typical geometrically non-linear model is written in terms of the displacement gradients:

$$\varepsilon = \frac{1}{2}(\nabla u_s + \nabla u_s^T + \nabla u_s^T \nabla u_s) \tag{7}$$

For small deformations, the last term on the right hand side is omitted to obtain a geometrically linear model. In this work we will consider geometrically nonlinear model (7) combined with both linear and nonlinear constitutive laws. The solid stress tensor  $\tau_s$  is given in terms of the second Piola-Kirchoff stress  $S$  :

$$\tau_s = (S \cdot (I + \nabla u_s)) \tag{8}$$

For the linear material model we employ the following constitute law relating the stress tensor to the strain tensor:

$$S = S_0 + C : \varepsilon \tag{9}$$

where  $C$  is the 4<sup>th</sup> order elasticity tensor and “:” stands for the double-dot tensor product,  $S_0$  and  $\varepsilon_0$  are initial stresses and strains respectively.

A hyperelastic material is defined by its strain energy density function  $W_s$  that is a function of the state of the strain in the body. For isotropic hyperelastic materials, the elastic strain energy can be written in terms of three invariants. Normally, the elastic deformation tensor is used (given by  $F_{el}$ ) along with the elastic right Cauchy-Green deformation tensor given by  $C_{el} = F_{el}^T F_{el}$ . One can then obtain the elastic Green-Lagrange strain tensor as  $\varepsilon_{el} = \frac{1}{2}(C_{el} - I)$  where  $I$  is the identity tensor. To describe a compressible model, we also require the elastic volume ratio defined by  $J_{el} = \det(F_{el})$ .

For the hyperelastic nonlinear material model, we employ the compressible neo-Hookean model:

$$W_s = \frac{1}{2} \mu (I_1 - 3) - \mu \log(J_{el}) + \frac{1}{2} \lambda [\log(J_{el})]^2 \quad S = \frac{\partial W_s}{\partial \varepsilon} \tag{10}$$

The weak variational form of the structural equations then becomes: Find the structure displacement  $u_s$  such that:

$$\int_{\Omega_f} \tau_s \cdot \varepsilon_s \, d\Omega_s = \int_{\Omega_f} F_s \cdot \phi_s \, d\Omega_s + \int_{\Gamma_s^N} t_s \cdot \phi_s \, d\Gamma - \int_{\Omega_f} \rho_s \frac{\partial^2 u}{\partial t^2} \cdot \phi_s \, d\Omega_s - \int_{\Gamma_I} (t_s^I - \tau_f \cdot n) \cdot \phi_s \, d\Gamma \tag{11}$$

### 2.3 Modeling the coupled fluid-structure system

In order to account for the changing nature of the fluid and solid sub-domains, one must define a dynamic mesh for the space discretization. However, to avoid extreme distortion, we choose to move the mesh independently of the fluid velocity in the interior of the fluid domain. Such a scheme, called arbitrary Lagrangian-Eulerian (ALE) formulation, is commonly applied when studying fluid-structure interaction [10, 16]. This choice allows us to use a Lagrangian framework for modelling the structure and a mixed formulation for modelling the fluid. In particular, we express the time derivatives as functions of Lagrangian reference coordinates, while the derivatives with respect to space are left as functions of the fixed Eulerian coordinates. To do this we define a mesh velocity  $w$  that describes the velocity of the mesh nodes as a time derivative of the deformation function. The ALE formulation for the fluid equation then becomes:

$$\rho_f \left( \frac{\partial u_f}{\partial t} \Big|_L + (u_f - w) \cdot \nabla_x u \right) + \nabla_d p = \nabla_x \cdot \tau + F$$

where  $L$  is the Lagrangian coordinate, and  $x$  the Eulerian coordinate.

## 2.4 Finite element discretization

Let the domain  $\Omega$  be partitioned into  $m$  non-overlapping sub-domains  $\{\Omega^i\}_{i=1}^m$  such that the intersection of any two sub-domains is empty, a vertex, or a collection of edges of the respective domains. In the latter case, we denote this interface by  $\Gamma^j$  which consists of individual common edges from the domains  $\Omega^i$  and  $\Omega^j$ . Over each subdomain, a fully coupled system is solved for the solution variables, namely, the velocity, the pressure, the stress vector and the structural displacements. The solution to the associated fluid-structure interaction problem is then achieved via an iterative strategy, where the systems of equations (11)-(12) along with the continuity equation are solved separately and in succession, always using the latest information, until convergence is reached.

## 3. Numerical Results

In this section, we will present the performance of the coupled algorithm applied to the model problem presented earlier. In all our experiments, the blood is modelled to enter the artery from the left side via a Poiseuille parabolic (see figure 2) profile whose amplitude is time dependent (in order to simulate a cardiac beat). In particular, we model the mean inlet velocity via:

$$u_{mean} = \frac{u_{max} t^2}{\sqrt{t^4 - 0.07t^2 + 0.0016}} \quad (12)$$

where  $u_{max} = 3.33$  cm/sec. The time dependence is taken from [17]. The channel height of the artery as indicated before was chosen to be  $100 \mu m$ . The fluid density and the dynamic viscosity were chosen to mimic blood properties to be  $\rho_f = 1050 \text{ kg/m}^3$  and  $\mu_f = 0.004 \text{ Pa sec}$  respectively.

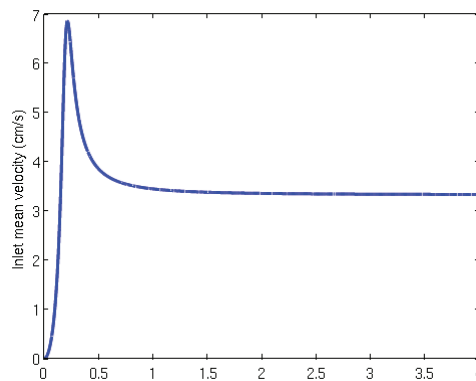


Figure 2. Plot of the mean inlet velocity

For modelling the structure, we consider three separate cases.

### Case I: Materially linear and geometrically linear (MLGL)

In this model we consider the arterial wall and the plaque to be modelled as geometrically linear and materially

linear. Hence the strain tensor is calculated as  $\varepsilon = \frac{1}{2}(\nabla u_s + \nabla u_s^T)$  and the isotropic solid stress tensor is

expressed in terms of the second Piola-Kirchhoff stress  $S$  as in (8) and (9). The values of density, Young's modulus and Poisson's ratio of the solid were chosen to be  $\rho_s = 1000 \text{ kg/m}^3$ ,  $E = 10^6 \text{ Pa}$  and  $\nu = 0.45$  respectively.



### Case II: Materially linear and geometrically nonlinear (MLGN)

In this model, we consider the arterial wall and the plaque to be both modelled as geometrically nonlinear and materially linear. In particular, we let the strain tensor to account for the geometric nonlinearity through the quadratic term in  $\varepsilon = \frac{1}{2}(\nabla u_s + \nabla u_s^T + \nabla u_s^T \nabla u_s)$ . The material model is chosen to be the same as in case I.

### Case III: Materially nonlinear and geometrically nonlinear (MNGN)

In this model, we consider the arterial wall and the plaque to be modelled as geometrically nonlinear as in Case II. However, the material is now considered to be hyperelastic compressible neo-Hookean model. We also choose the arterial wall properties to be different from the properties of the plaque. In particular we choose the following values for the arterial wall properties  $\rho_s = 1000 \text{ kg/m}^3$ ,  $\lambda = 3.1 \times 10^6 \text{ Pa}$ ,  $\mu = 3.45 \times 10^5 \text{ Pa}$  and for the plaque we choose  $\rho_s = 1000 \text{ kg/m}^3$ ,  $\mu = 6.2 \times 10^6 \text{ Pa}$ ,  $\lambda = 20\mu - \frac{2}{3}\mu \text{ Pa}$ . In order to be consistent in the values, we choose the Young's modulus and Poisson ratio values to correspond to the values of the Lamé constants:

$$\mu = \frac{E}{2(1+\nu)}, \quad \lambda = \frac{E\nu}{(1+\nu)(1-2\nu)}$$

The prescribed inlet velocity profile attains a maximum value at about  $t=0.215$  sec. The velocity and stress distributions at four different times are presented in figure 3 for the MNGN model. Figure 4 illustrates the surface pressure and velocity profiles at  $t=0.215$  sec. The maximum values of the von Mises stress and the velocity values for each of these simulations is illustrated in figure 5. Both the multiphysics simulations as well as the maximum values clearly show the importance of including the nonlinear effects in the material and the geometry. The values in figure 5 clearly indicate that the nonlinearity of the geometry increases the value of the stresses and the maximum velocity. These also create multiple recirculation zones with the model in MNGN creating vortex formation (see figure 3) which could potential lead to very high shear stresses near the throat of the plaque. The later can induce thrombosis which can totally block blood flow to the heart or brain. Detection and quantification of such vortices is very valuable and can serve as the basis for surgical intervention.

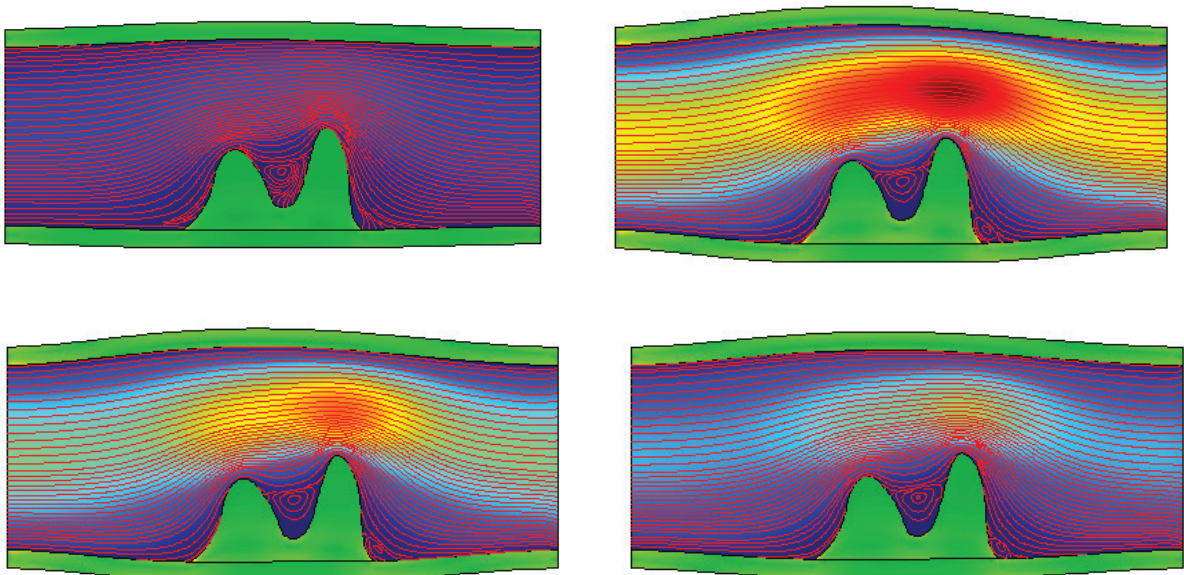


Figure 3: The surface von Mises Stress along with streamlines of spatial velocity field shown at times  $t=0.1$  sec (top-left),  $t=0.215$  sec (top-right),  $t=0.3$  sec (bottom-left) and  $t=4$  sec (bottom-right) for the MNGN model.

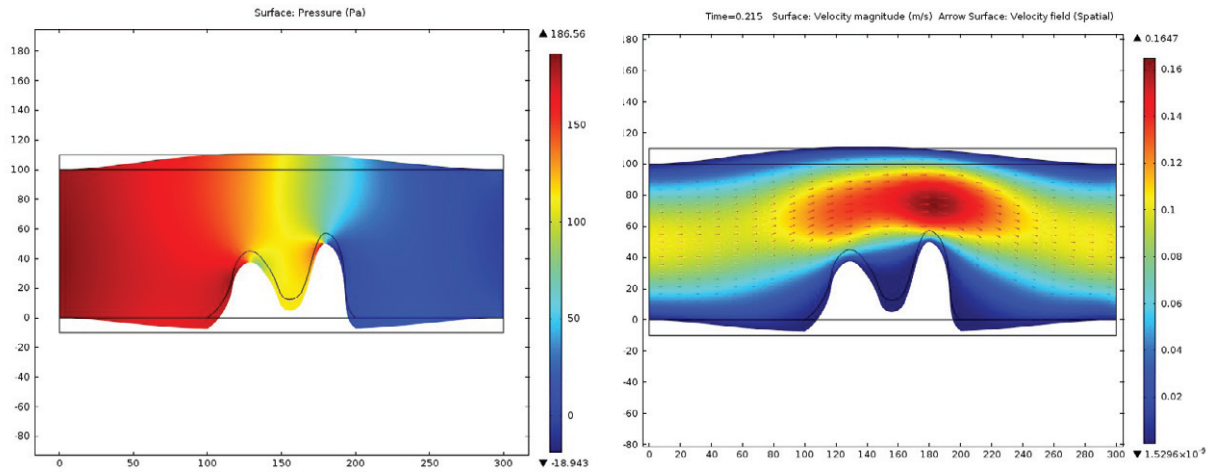


Figure 4: Surface pressure distribution at t=0.215 sec and velocity profile for MNGN models

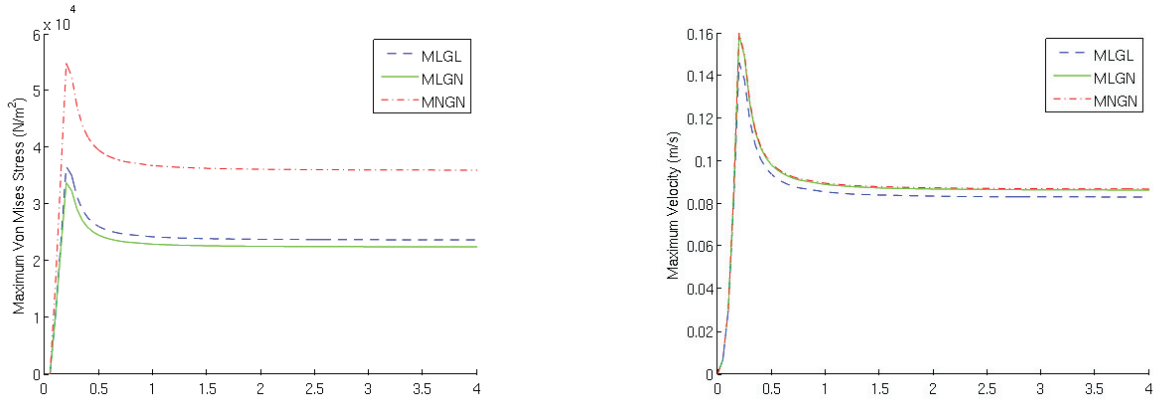


Figure 5: Comparison of the maximum Von Mises Stresses and Maximum Velocity profiles for all three models

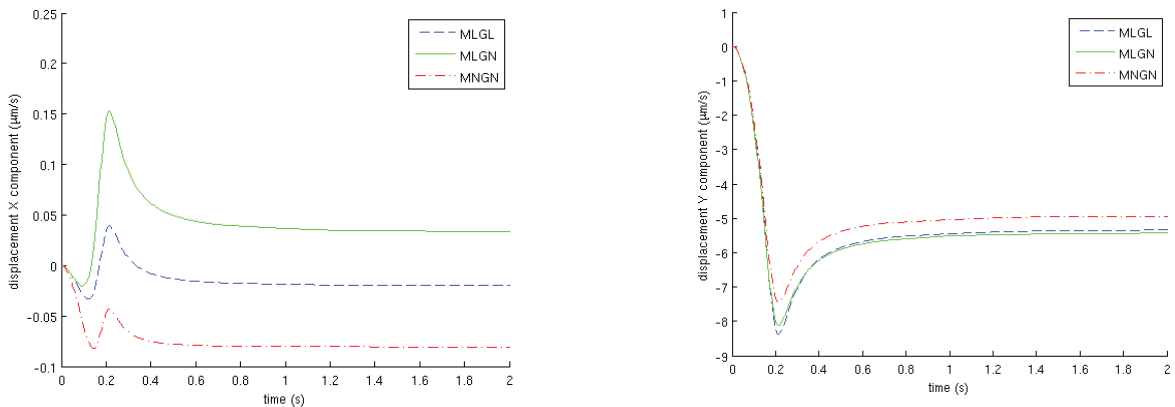


Figure 6: A comparison of the in x- and y-displacements of the point (136, 41) micrometers for the three models



At the coordinate (136, 41) micrometers in the computational domain which was on the surface of the first hill of the plaque, we measured the displacement and the velocity profiles for all times. Specifically, Figure 6 illustrates the x- and y- components of the structural displacement. Not only is the movement of the plaque evident from these plots but also it indicates the influence of the nonlinear effects in material and geometry on controlling the displacement. The completely nonlinear model (MNGN) shows the extreme behavior of the three models.

#### 4. Conclusion

In this paper, we presented the mathematical modeling and simulation of a fluid-structure interaction algorithm applied to a multiphysics application involving atherosclerotic arteries. The model incorporated both geometric nonlinearity and material nonlinearity for the arterial wall and the plaque that interacted with unsteady blood flow. The results clearly indicate the generation of recirculation zones at various locations near the plaque which could potentially enhance the risk of the formation of a clot. Three separate models were considered in this work and their influence on the behavior of the plaque was studied. The results indicate that a plaque modeled as a materially nonlinear and geometrically nonlinear shows evidence of recirculation that is different from those that are modeled using linear models. Such studies are essential to get a good insight into the risk of rupture of a plaque. In this work, we considered the flow to be Newtonian. In the future study we plan to consider effects of non-Newtonian rheological properties incorporated along with this materially and geometrically nonlinear model developed and presented in this paper.

#### References

1. C. Bernardi, Y. Maday and A. Patera, "Domain decomposition by the mortar element method", *Asymptotic and numerical methods for partial differential equation with critical parameters*. H.K. et al. eds, Reidel, Dordrecht, pp. 269-286, 1993.
2. F. Ben Belgacem, "The mortar finite element method with Lagrange Multipliers", *Numer. Math.*, vol. 84(2), pp. 173-197, 1999.
3. P. Seshaiyer and M.Suri, "hp submeshing via non-conforming finite element methods", *Comput. Meth. Appl. Mech. Eng.*, vol. 189, pp. 1011-1030, 2000.
4. P. Seshaiyer, "Stability and convergence of non-conforming hp finite element methods", *Computers and Mathematics with applications*, 46: 165-182 (2003).
5. F. Ben Belgacem, L.K. Chilton and P. Seshaiyer, "The hp-Mortar Finite Element Method for Mixed elasticity and Stokes Problems", *Comput. Math. Appl.*, vol. 46, pp. 35-55, 2003.
6. E. Aulisa, S. Manservigi and P. Seshaiyer, "A computational multilevel approach for solving 2D Navier-Stokes equations over non-matching grids", *{Comput. Meth. Appl. Mech. Eng.}*, vol 195, pp 4604-4616, 2006.
7. Y.C. Chang, T.Y. Hou, B. Merriman, S. Osher, "A Level Set Formulation of Eulerian Interface Capturing Methods for Incompressible Fluid Flows", *Journal of Computational Physics*, 124(2): 449-464 (1996).
8. F. P. T. Baaijens, "A fictitious domain/mortar element method for fluid-structure interaction", *International Journal for Numerical Methods in Fluids*, 35: 743-761 (2001).
9. R. Glowinski et. al., "A fictitious domain approach to the direct numerical simulation of incompressible viscous flow past moving rigid bodies: Application to particulate Flow", *Journal of Computational Physics*, 169(2), 363-426 (2001).
10. E.W. Swim and P. Seshaiyer, "A nonconforming finite element method for fluid-structure interaction problems", *Comput. Meth. Appl. Mech. Eng.*, vol. 195(17-18), pp. 2088-2099, 2006.
11. E. Aulisa, A. Cervone, S. Manservigi and P. Seshaiyer, "A multilevel domain decomposition approach for studying coupled flow applications", *Communication in Computational Physics*, 6: 319-341 (2009).
12. C. Peskin, *Numerical Analysis of Blood Flow in the Heart*. *Journal of Computational Physics*, 25: 220-252 (1977).
13. P.M. Rothwell et. al., "Analysis of pooled data from the randomized controlled trials of endarterectomy for symptomatic carotid stenosis", *Lancet* 361:107-116 (2003).
14. M. Bathe and R. D. Kamm, "A fluid-structure interaction finite element analysis of pulsatile blood flow through a compliant stenotic artery", *ASME Journal of Biomechanical Engineering*, 121: 361-369 (1999).
15. D. Tang et. al., "Effect of a lipid pool on stress/strain distributions in stenotic arteries: 3D fluid-structure (FSI) models", *Journal of Biomechanical Engineering*, 126: 363-370 (2004).
16. J. Donea, S. Giuliani, J.P. Halleux, "An arbitrary Lagrangian-Eulerian finite element method for transient dynamic fluid-structure interactions", *Computer Methods in Applied Mechanics and Engineering*, 33:689-723 (1982).
17. Zhi-Yong Li, PhD; Simon P.S. Howarth, MRCS, Eng ; Tjun Tang, MRCS Jonathan H. Gillard. How Critical Is Fibrous Cap Thickness to Carotid Plaque Stability ? A Flow Plaque Interaction Model. *Stroke* 37 : 1195-1196, 2006.